# Measurement of $\pi^+\pi^-$ Photoproduction in Double-Polarization Experiments using CLAS

## Prospectus of Dissertation

Charles Hanretty

Department of Physics, Florida State University

November 7, 2006

Major Professor : _____
Committee Member : _____
Committee Member : _____
Committee Member : _____
Committee Member : _____

## Abstract

The proposed research activities focus on the investigation of nuclear properties using a polarized tagged photon beam and a polarized target. Photon-induced reactions on the nucleon form a rich source of information for the baryon spectrum. Spectroscopic predictions are not possible in the non-perturbative regime of Quantum Chromodynamics (QCD). For this reason, effective theories and models have been developed to determine the masses, couplings, and decay widths of resonances. Various constituent quark models (CQMs) based on three quark degrees of freedom predict numerous baryon resonances that have not been experimentally verified and are thus "missing". The persistent non-observation of these states would present a big problem as the models would have failed to describe physical reality. CQMs predict strong couplings of these states to $\gamma$N as well as to N$\eta$, N$\eta'$ or $\Delta\pi$ making photoproduction experiments a promising method to find these missing resonances. Previous analyses of unpolarized data show the importance of polarization observables because some resonances reveal themselves more clearly in the interference with more dominant amplitudes. In addition, the determination of resonant contributions based on unpolarized data is not unique and requires further constraints provided by single- and double polarization observables. A linearly- and circularly-polarized photon beam will be incident on a frozen-spin butanol target in Jefferson Lab's Hall B CLAS detector located in Newport News, Va. This detector allows the target to be polarized both longitudinally as well as transversely giving rise to 15 polarization observables in $\pi^+\pi^-$ production. The proposed research will determine at least one of the above observables and thus, will shed some light on the problem of the missing baryon resonances serving to better understand the properties of these states.

## Introduction

A problem encountered in baryon spectroscopy is the fact that excited states of the nucleon are not seen as cleanly separated spectral lines like in the case of a hydrogen atom, but as broadly overlapping resonances which decay into multiple final states including both mesons and baryons. These overlapping resonances can sometimes be better identified through their interference with other dominant amplitudes. By determining the polarization observables in polarization experiments, one can isolate these interference effects, providing better access to resonance contributions.

Currently, the best method for predicting the masses, widths, and other decay properties of baryon states is by using Constituent Quark Models (CQM's) (Fig. 1) since the QCD Lagrangian cannot be solved for such low energies. These models in the past have shown good agreement with experimental data making them a favorable tool for predicting baryon states [1] [12] [13]. Despite the fact that these calculations only give us suggestions, they are the only source of information available to us on how to produce these resonances. Presumably within the next five years, given the latest progress in the field, more accurate predictions from lattice-QCD calculations will be available derived from a fundamental quantum field theory. At that time, it will be very important to have the necessary data at hand, which consequently have to be taken now. Whereas we do not intend to test these CQM's, they do give us an idea of where to look for exciting physics and therefore we seek to obtain data regarding these predicted states.

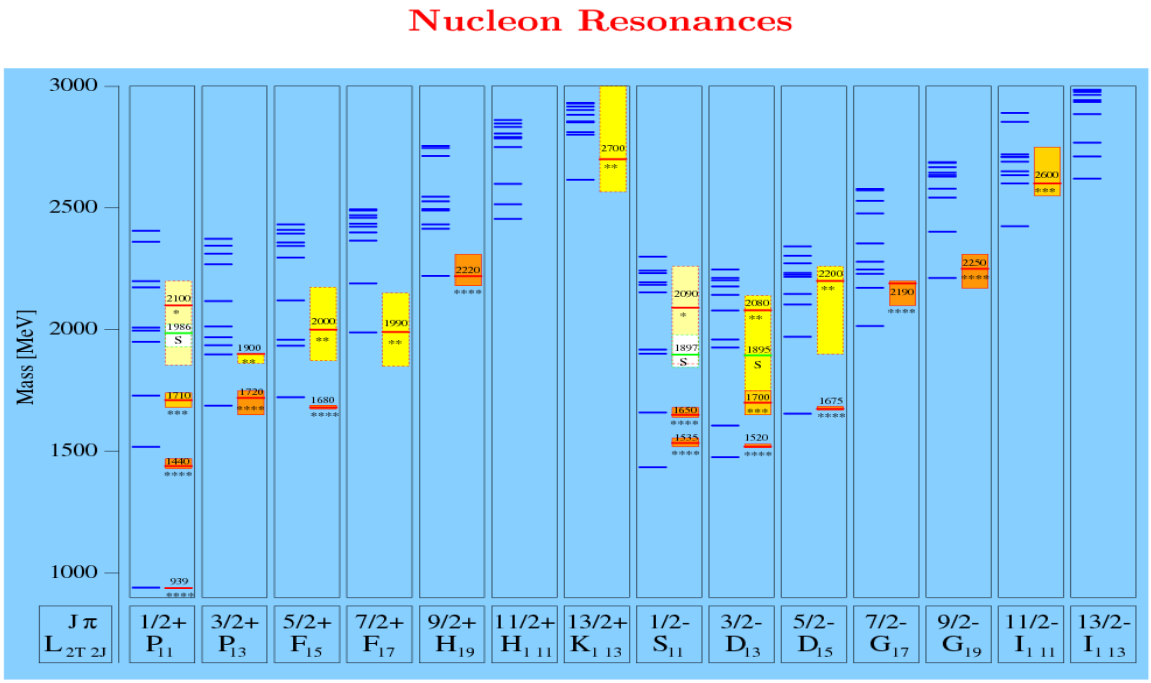


*Fig 1: N* resonances. The left side of each column shows model predictions [1] while the right side represents experimental findings. The number of *'s indicates the ranking of the state according to the PDG (a four star state being well established).*

CQM's have been successful at predicting the properties (such as the mass, width, and the decay properties) of low-mass baryon resonances, at higher energies they predict many resonances that have not yet been experimentally verified. There are several possibilities as to why there are no experimental findings on these baryon states:

- If these missing resonances do not couple to N$\pi$ they would not be seen in N$\pi$ elastic scattering experiments; most of our knowledge on baryon states stems from this kind of experiment.

- Existing photoproduction data, on which data analysis has just recently begun, covers mainly a mass range up to 1800 MeV/$c^2$. The missing resonance problem appears essentially at and above 1900 MeV/$c^2$.

- Polarization observables for photoproduction have been previously measured at GRAAL (Grenoble, France), LEGS (BNL, USA), ELSA (Bonn, Germany), and MAMI (Mainz, Germany), but at low energies. When the energy is increased, these resonances overlap more strongly making the determination of the polarization observables even more important to the analysis helping to distinguish between different resonances.

- Lastly, the often explored channels contain only a single meson in the final state (e.g. N$\pi$, N$\eta$, N$\omega$).

Looking at two-meson final states can be of more use because in spite of the fact that these high-lying missing states may not couple strongly to $\pi$p or $\gamma$p, they may be observed in a decay chain as an intermediate state leading to a final state with two mesons (e.g. $\gamma p \rightarrow N^* \rightarrow \Delta^0\pi^+ \rightarrow p\pi^+\pi^-$).

Past experiments on this matter have focused on quasi 2-body final states. It has recently been indicated, however, that looking at a 3-body final states has great potential for revealing the high-mass missing states because they account for most of the cross section above W ≈ 1.7 GeV. These missing states are predicted to decay into particles with higher masses (excited intermediate states) rather than a final state characterized by a meson and a ground-state nucleon. The widths of these missing states are at least 150 MeV. Calculations of the decays of these resonances into two-particle channels (like N$\pi$) result in very narrow particle widths, meaning the majority of the decays involve more than just a two-body final state.

## Motivation to Study the Reaction $\gamma p \rightarrow p\pi^+\pi^-$

In the study of missing baryon resonances, a key tool is the investigation of double-pion photoproduction. In the low-energy range for example, the $P_{11}$ (1440) (Roper Resonance) and its properties can be investigated. In the proposed research, the plan is to analyze the $\pi^+\pi^-$ jointly with polarization data on single-pion photoproduction, which was proposed in E03-105 [6] and E04-102 [7]. This will help to obtain a better understanding of the $P_{11}$ (1440). Furthermore at higher energies, a group of negative-parity $\Delta$-states with masses around 1900 MeV can be studied for which only weak evidence exists so far. Their verification would be in contradiction with quark-model calculations predicting these states at significantly higher masses.

This, however requires a detector with a large angular acceptance like the CLAS spectrometer in JLab's Hall B (Fig. 2). This reaction also requires a much more involved analysis due to large non-resonant background contributions. Despite the difficulty of the analysis, the reaction $\gamma p \rightarrow p\pi^+\pi^-$ is a promising reaction for the search of states that decay into $\Delta\pi$ and p$\rho$ due to the large branching fraction of $\Delta \rightarrow N\pi$ and $\rho \rightarrow \pi^+\pi^-$. Current, unpolarized data on double-pion photoproduction leads to ambiguous determinations of the resonances contributions. The Frozen Spin Target (FROST) at JLab used along with a polarized electron beam (leading to a polarized photon beam) will allow the

determination of polarization observables resulting in a clearer understanding of the missing resonances.

## Experiment

### CEBAF Large Acceptance Spectrometer (CLAS)

The CLAS spectrometer is divided into six sectors by a superconducting, toroidal magnet. Immediately surrounding the target area is the new start counter made up of a set of 24 scintillators in six sectors. The purpose of the start counter is to provide a time stamp for the start of a reaction. This time can then be matched to a certain tagged photon. Moving from the inside of CLAS to the outside, there is another set of scintillators following the drift chambers. These scintillators are the time-of-flight scintillators which provide timing information to be used with the particle tracks and the start counter in order to find the velocities and energies of the outgoing particles. Finally, in the forward region of CLAS are the calorimeters which are primarily used for detection of neutral particles.

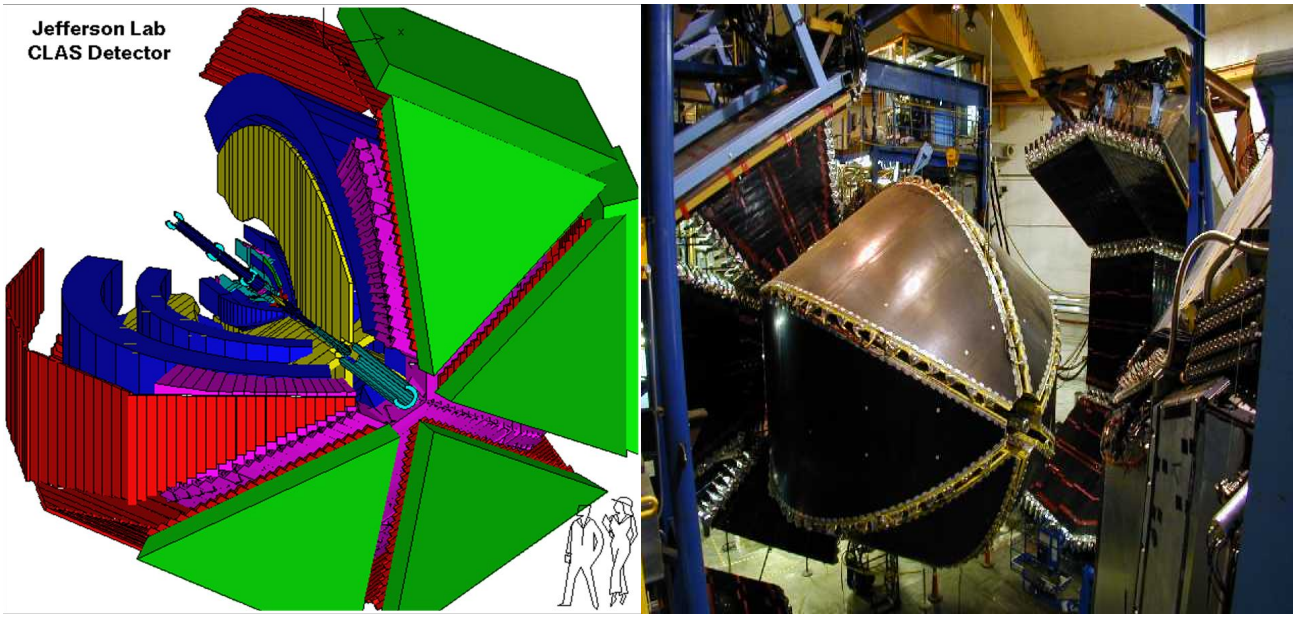


*Fig 2: JLab's CLAS detector. The yellow is the torus magnet, the blue regions the drift chambers. Behind that in purple, the Cerenkov counter followed by the time-of-flight counter. Finally in green is the electromagnetic calorimeter. To the right is a picture of CLAS when open.*

### Tagged Photon Beams

When it comes to producing tagged photon beams for photo-induced reactions, there are generally two approaches. The first method is employed at SPring-8, Japan, and GRAAL and uses a laser light along with an electron beam. A polarized photon beam is created by Compton backscattering of the laser light off an electron beam. The backscattered photons receive their polarization naturally from the laser beam and while this process doesn't require much effort, the luminosity is very limited by the interaction of the laser with the circulating electron beam.

At institutions such as ELSA and JLab, the method of creating tagged and polarized photon uses bremsstrahlung radiation. This process utilizes an electron beam incident on a radiator (gold foil or diamond) which leads to a photon beam with a higher luminosity than the previous process.

## Linearly-Polarized Photon Beams

The broad-range tagging facility in Hall B at JLab has reliably provided two kinds of tagged-photon beams. A well oriented diamond radiator is used for production of a linearly-polarized photon beam by means of coherent bremsstrahlung radiation. Generally the range of photon energies that can be tagged at JLab covers 20% to 95% of the incident electron beam energy, however over 80% of the linearly-polarized photon flux resides in a 200 MeV wide energy interval. The degree of photon polarization is a function of the fractional photon beam energy ($k = E_\gamma / E_{e^-}$) and collimation, with the ability to reach values of 80% to 90% (Fig. 3). The degree of polarization will increase with a lower fractional energy but is fairly constant over a 200 MeV energy range near the coherent edge.

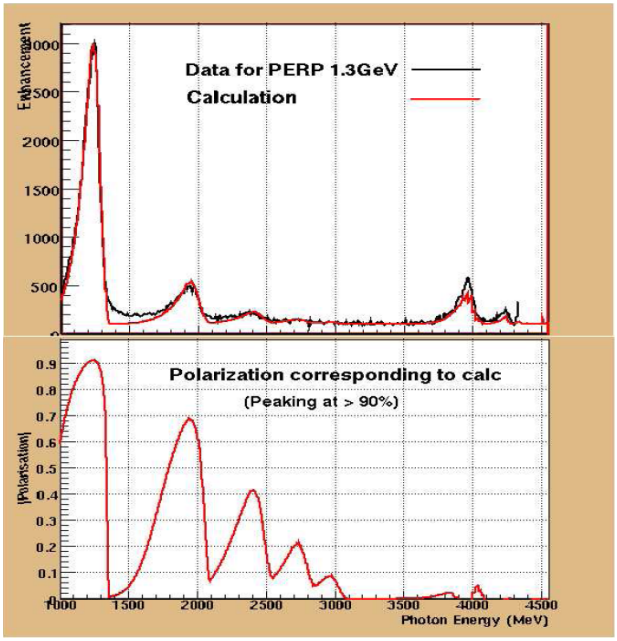


*Fig 3: The plots above show the high degree of photon polarization possible in Hall B. The data came from the g8b experiment conducted in summer 2005. The plot shows that the degree of photon polarization can reach values of over 90% .*

## Circularly-Polarized Photon Beams

A circularly-polarized photon beam is produced using a beam of longitudinally polarized electrons incident on a bremsstrahlung radiator made of gold plated on a thin carbon foil. The degree of polarization once again depends on the ratio $k = E_\gamma / E_{e^-}$. The values of photon polarization range from 60% to 99% of the incident electron beam polarization for photon energies between 50% and 95% of the incident electron energy. The polarization is approximately given by Ref. [4]:

$$P_\odot = P_e \cdot \frac{4k - k^2}{4 - 4k + 3k^2}$$

## Polarized Targets

### Current Polarized Target

The current polarized $NH_3$ target for use with the CLAS spectrometer is a dynamically polarized target that was used for electroproduction experiments. The polarizing magnet utilizes a pair of 5 T Helmholtz coils resulting in longitudinal polarization. This magnet, however, is large and requires the target to sit inside of the magnet limiting the available opening to 55 degrees in the forward direction. This means that because the target sits inside a large magnet, there is a significant portion of outgoing particles that are blocked.

### Frozen-Spin Target (FROST)

The FROST target (Fig. 4 and Fig. 5) uses butanol ($C_4H_9OH$) as the target material to produce both longitudinal as well as transverse polarization with a minimum amount of material between the target and CLAS. Use of this target will lead to high-quality data for the channels to be analyzed. There are currently five proposals approved by the JLab PAC for use with this target. Four focus on single-meson photoproduction [5-8] and one on double pion photoproduction [9].

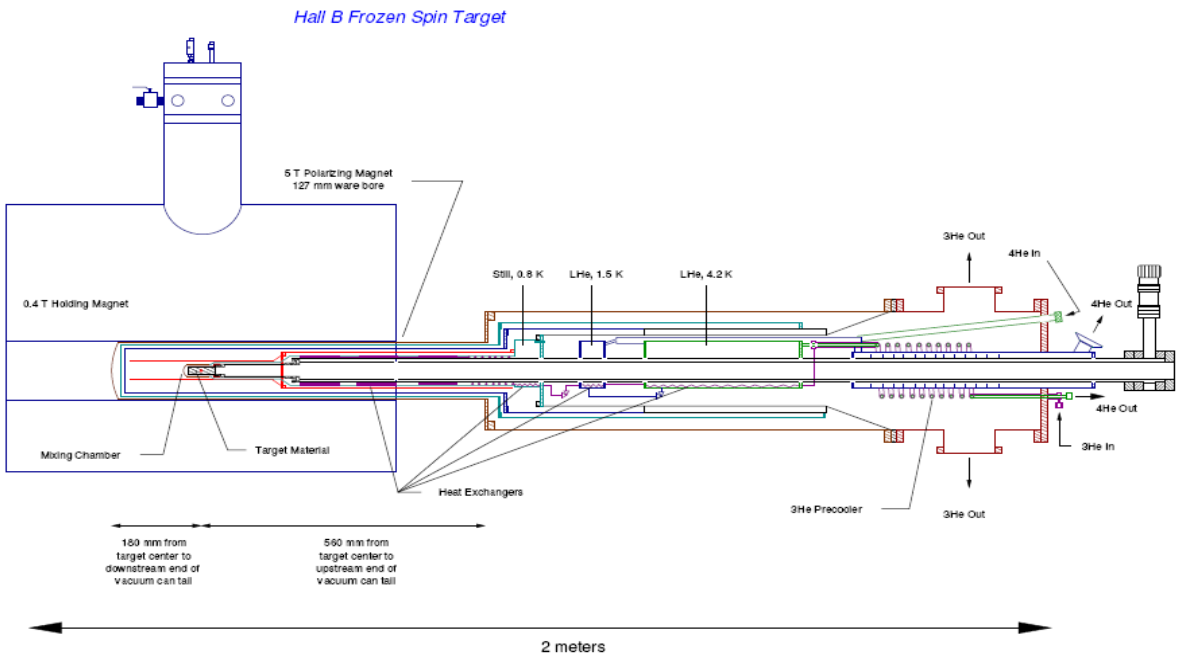


*Fig 4: A diagram of the FROST target. FROST is shown here with the target material in the polarizing magnet (large object on the left).*

This FROST target will operate in a position such that the target cell will be in the geometrical center of CLAS. The target cooling system will be a horizontal piece 200 cm in length with a maximum diameter of 25 cm. Since the material between the target and the detectors needs to be minimal, the target will be polarized outside of CLAS and during data-taking, reside in a magnetic holding field. The polarizing magnet will dynamically polarize the target material through microwave irradiation in a strong magnetic field of 5 T in an environment of 0.5 K. In the process of dynamic polarization, free electrons are polarized by a strong magnetic field and then microwaves are used to transfer that polarization to the nucleon. After the target has attained the maximum degree of polarization, the dilution refrigerator and holding magnet will be turned on. This "freezes" the spin of the protons and preserves it in a 0.5 T magnetic field at a temperature of 50 mK. The target will then be moved into

position in the center of CLAS. A butanol target with an initial proton polarization of 90% has a relaxing time of several days under this procedure giving sufficient time for a useful polarized target experiment. Once the target's polarization has decomposed down to about 50-60%, the target is then taken out of CLAS, put back into the high magnetic field and repolarized.

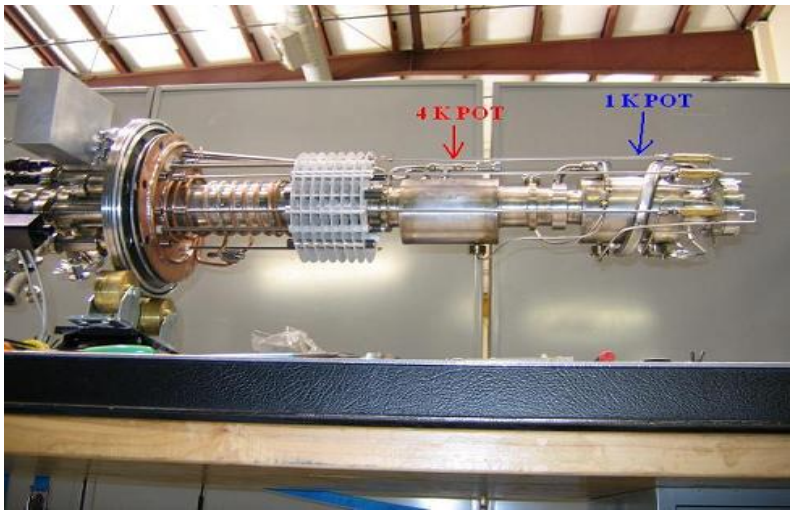


*Fig 5: The fully assembled pre-cooler for FROST. Here temperatures of about 1K are reached by using liquid helium. The cylinder that goes through the center of the pre-cooler is a concentric heat exchanger. Constructed and assembled Summer 2006.*

The target cell itself is 50 mm in length and 15 mm in diameter. The target material will be butanol ($C_4H_9OH$) with a dilution factor (fraction of polarizable nucleons) of approximately 13.5%. A similar target has been constructed and used at the German photonuclear facilities such as Mainz and Bonn with maximum polarizations of 85% to 95% [10, 11].

## Polarizing Magnet

The polarizing magnet used with the FROST target is a horizontal superconducting solenoid magnet capable of producing a field of 5 T with a hole 130 mm in diameter bored through it. This magnet, purchased form Cryomagnetics Inc., underwent a precise NMR measurement upon its arrival at JLab. This test confirmed that the homogeneity of the magnetic field within the target volume (15 mm in diameter and 50 mm in length) is better than 40 ppm.

## Dilution Refrigerator

To freeze the spin of the proton, temperatures of about 50 mK are necessary (which cannot be obtained through the normal use of liquid helium). Therefore, a process called dilution refrigeration must be used to reach this low temperature. Dilution refrigeration works on the principle that when a mixture of the two stable isotopes of helium, $He_3$ and $He_4$, is cooled below a critical temperature, it separates into two phases. The lighter "concentrated phase" is rich in $He_3$, and the heavier "dilute phase" is rich in $He_4$. The concentration of $He_3$ in each phase is temperature-dependent. Since the enthalpy of the $He_3$ in the two phases is different, the "evaporation" of $He_3$ from the concentrated phase into the dilute phase provides highly effective cooling. In a gross simplification, the concentrated phase of the mixture is pretty much liquid $He_3$, and the dilute phase is essentially $He_3$ gas. The evaporation of the $He_3$ from the "liquid" phase to the "gas" phase cools the sample. This process works even at the lowest temperatures because the equilibrium concentration of $He_3$ in the dilute phase is finite even at zero temperature.

The FROST dilution refrigerator (Fig. 6) utilizes both $He_3$ and $He_4$ to reach a target temperature of 50 mK. The major components relevant to this process are the concentric heat exchanger (four concentric cylinders increasing in radius so that there are three open space between them), the 4 K Pot, the 1 K Pot, the mixing chamber and the still. The $He_4$ comes in from the pump cart into the 4 K Pot. In the 4 K Pot there is a valve that allows some of the $He_4$ to flow to the outer channel of the concentric heat exchanger. Another valve allows some of the $He_4$ to flow from the 4 K Pot to the 1 K Pot. Incoming $He_3$ travels through the middle space of the concentric heat exchanger, being cooled by the $He_4$ from the 4 K Pot and $He_4$ leaving the 1 K Pot traveling through the inner space of the concentric heat exchanger. The $He_3$ then goes into the 1 K Pot where it does not mix with the $He_4$. Then the $He_3$ goes through a condenser, is cooled by the still and moves on to the mixing chamber. In the mixing chamber is both $He_3$ and $He_4$ which are experiencing a phase separation because the temperature is below 0.86 K. The $He_3$ (in its concentrated form) in the mixing chamber sits on top of the $He_4$. The $He_3$ then dilutes the $He_4$ which requires energy to do. This draws heat from the target, making it possible to attain temperatures of 50 mK. For this process to continue, $He_3$ that dissolved into the $He_4$ must be pumped off to replenish the $He_3$ in the mixing chamber. This is done in the still where, at such a temperature, $He_3$ evaporates 1000 times more than the $He_4$. The $He_3$ is then pumped off, sent through pumps which compress it and purify it and then sent back to the dilution refrigerator.

During the running of the experiment, the photon beam will impart a heat load of about 1 $\mu$W. This means that when FROST is in frozen spin mode at 0.5 T and 50 mK, the refrigerator will provide cooling power of a few $\mu$W.

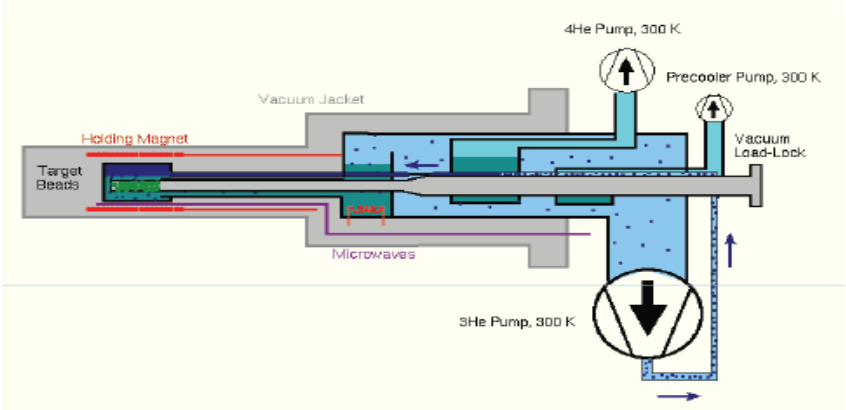


*Fig 6: A cartoon of the dilution refrigerator. Most dilution refrigerators are vertical, but in order for FROST to be used with CLAS, a horizontal dilution refrigerator was needed.*

## Holding Magnet

As seen in previous polarized target experiments, the apparatus providing the magnetic field can affect the data by blocking some of the particles from the scattering reaction. Since FROST uses a smaller magnet to preserve the polarization, this internal holding system should be as transparent as possible to any outgoing particles. This requirement limits the amount of conductor that can be used to produce the field resulting in a field of lower intensity. The current design of the holding magnet (both the longitudinal and transverse holding magnet) will produce a field of 0.5 T with a homogeneity of better than 1% within the target cell volume. This low variance in the magnetic field will allow the degree of polarization to be closely monitored during the experimental runs.

Since this experiment requires both a longitudinal and a transversely polarized target, two different magnet designs are needed. The longitudinal holding magnet (Fig. 7) is a solenoid in design.

According to simulations, three layers of NbTi superconducting wire (0.112 mm in diameter) are best suited for our purpose. These three layers will provide a central field intensity of up to 0.5 T with a homogeneity over the entire target of less than 0.5%. Tests of a prototype of this holding magnet have confirmed the results of the simulation. The design for the transverse holding magnet (Fig. 7) is a dipole magnet with racetrack shaped coils. There are two coils, one on top of the cylinder and one on the bottom with both coils being made from one continuous NbTi superconducting wire. The position of the coils in CLAS will be such that they are as much as possible in the shadows of the CLAS torus in order to minimize the loss of acceptance. This holding coil will produce a field of 0.5 T with a homogeneity of better than 0.8% using three layers of superconducting wire.

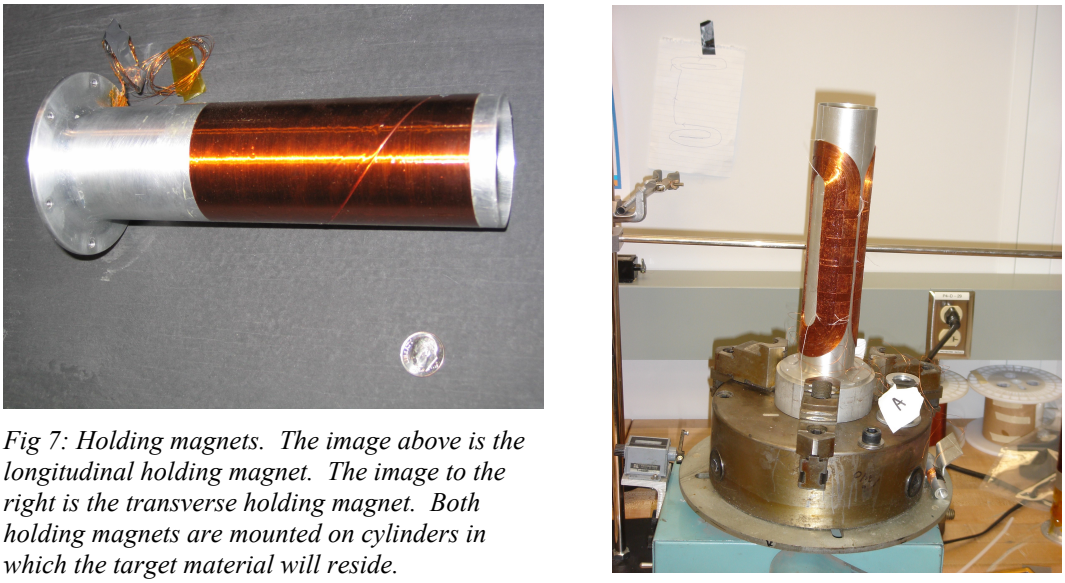

*Fig 7: Holding magnets. The image above is the longitudinal holding magnet. The image to the right is the transverse holding magnet. Both holding magnets are mounted on cylinders in which the target material will reside.*

I began work on the transverse holding magnet the summer of 2005. I developed the methods and determined the materials to be used for constructing this superconducting magnet as a magnet like this has never been used before. The placement of the wire on the surface of the cylinder as well as the placement of the coils themselves relative to each other are important as the two coils must produce magnetic fields that work together to produce a uniform field perpendicular to the axis of the cylinder. For this reason, the homogeneity of the magnetic field is slightly worse than the homogeneity of the solenoid magnet. As mentioned before the design of the magnet utilized a racetrack shaped design made of the same kind of wire with a coil on top and a coil on bottom. The two coils, however, were not made of one continuous wire, but with each coil being made of its own individual wire. This was done in case one coil failed, the whole apparatus would not have to be made again. The cylinder on which the coils were placed had grooves cut into it so that the first layer of wire could sit in securely on the surface. Each subsequent layer (there are three layers per coil) then sits in the grooves provided by the previous layer. The first layer had 186 turns, the second 166, and the third 144. These wires were placed in the grooves using a system of pulleys that kept a small amount of tension on the wire with the cylinder resting on a manually rotating table. Once the wire was placed in its position, a soldering iron was used in order to melt the wire through a layer of purified paraffin. This design, however, was put aside due to overall modifications of the FROST design. The modified holding magnet uses a more automated system and epoxy instead of purified paraffin. This prototype is presently undergoing testing.

Work done during the summer of 2006 consisted of fabrication of parts as well as assembly of FROST. The pre-cooler and dilution refrigerator were the first to be constructed. The inner tubes for the

concentric heat exchanger were machined and cleaned while the pump cart was prepared and the pumps plumbed. The gas handling system and the heat exchangers were next to be machined in-house and assembled.

Having each part that goes into FROST be leak tight is an obvious must. Because of this highly important requirement, each part of FROST was immediately leak-checked after any welds or joints were made. These leak checks were performed using a helium spectrometer. The piece was hooked up to a high-vacuum system and pumped down to about $10^{-5}$ Torr. Once this pressure was reached, the helium spectrometer was turned on and a very weak stream of helium gas was sprayed on the joints to see if any was sucked through to the spectrometer. Once a piece was deemed leak-tight, it could then be attached as a green-lit piece of FROST. My role in this process was the fabrication of parts for the construction itself, machining parts for the gas handling system, and machining valves, heat exchangers, tubing, supports, and flanges on the lathe and mill. I also worked on the assembly of parts, and leak-checking.

## Analysis

In the energy regime under study, the broad and overlapping resonances cause problems in the analysis. Thus polarization observables, which are sensitive to small resonant contributions, will be very helpful in the evaluation of N* parameters.

The total cross section is given by (the polarization of the recoiling nucleon is ignored) [3]: (Eq. 1)

$$\begin{aligned} I \;=\; I_0 \{\, ( 1 \,+\, \vec{\Lambda}_i \cdot \vec{\mathbf{P}} \,) \\ &+\, \delta_\odot \, ( \mathbf{I}^\odot \,+\, \vec{\Lambda}_i \cdot \vec{\mathbf{P}}^{\,\odot} \,) \\ &+\, \delta_l \, [ \sin 2\beta \, ( \, \mathbf{I}^{\mathbf{s}} \,+\, \vec{\Lambda}_i \cdot \vec{\mathbf{P}}^{\,\mathbf{s}} \,) \\ &\qquad \cos 2\beta \, ( \, \mathbf{I}^{\mathbf{c}} \,+\, \vec{\Lambda}_i \cdot \vec{\mathbf{P}}^{\,\mathbf{c}} \,) \,] \,\} \end{aligned}$$

Where I is the reaction rate, $I_0$ is the unpolarized reaction rate, **P** represents the polarization asymmetry that arises if at least the target nucleon is polarized and $\boldsymbol{\Lambda_i}$ denotes the polarization of the initial nucleon. The degree of circular polarization of the photon beam is denoted by $\delta_\odot$, the degree of linear polarization is denoted by $\delta_l$ and $\beta$ denotes the orientation of the linear polarization. The $\mathbf{I}^{\,s}$ and $\mathbf{I}^{\,c}$ are the sine and cosine contributions of the observables arising from the use of a polarized photon beam. These polarization observables can be isolated through the use of four polarization settings:

- beam circularly polarized, target transversely polarized
- beam circularly polarized, target longitudinally polarized
- beam linearly polarized, target longitudinally polarized
- beam linearly polarized, target transversely polarized

Example: polarization
In the following, → and ← indicate circular polarization of the beam in its two possible settings while ⇐ and ⇒ indicate longitudinal target polarization parallel and anti-parallel to the beam. Then Eq. 1 yields: (Eq. 2)

$$(\rightarrow\Rightarrow - \leftarrow\Rightarrow) := \frac{\mathrm{d}\,\sigma(\rightarrow\Rightarrow)}{\mathrm{d}\,x_i} - \frac{\mathrm{d}\,\sigma(\leftarrow\Rightarrow)}{\mathrm{d}\,x_i} = 2\cdot\sigma_0\,\{\delta_\odot\,(\mathbf{I}^\odot + \Lambda_z\cdot\mathbf{P}_\mathbf{z}^\odot)\}$$
$$(\leftarrow\Leftarrow - \rightarrow\Leftarrow) := \frac{\mathrm{d}\,\sigma(\leftarrow\Leftarrow)}{\mathrm{d}\,x_i} - \frac{\mathrm{d}\,\sigma(\rightarrow\Leftarrow)}{\mathrm{d}\,x_i} = 2\cdot\sigma_0\,\{\delta_\odot\,(-\mathbf{I}^\odot + \Lambda_z\cdot\mathbf{P}_\mathbf{z}^\odot)\}$$

The above shows the result of flipping only the polarization of the beam. It has to be pointed out that all observables of Eq. 2 are 5-fold differential and thus $x_i$ stands for the 5 independent variables. It is obvious from this that only changing the polarization of the beam is not sufficient to isolate and extract the polarization observable $\mathbf{P_z^\odot}$. Therefore it is necessary to have all four polarization configurations such that $\mathbf{P_z^\odot}$ can be determined:

$$(\rightarrow\Rightarrow - \leftarrow\Rightarrow) + (\leftarrow\Leftarrow - \rightarrow\Leftarrow) := \frac{\mathrm{d}\,\sigma_{3/2}}{\mathrm{d}\,x_i} - \frac{\mathrm{d}\,\sigma_{1/2}}{\mathrm{d}\,x_i} = 4\cdot\sigma_0\cdot\delta_\odot\cdot(\Lambda_z\cdot\mathbf{P}_\mathbf{z}^\odot)$$

## Sensitivity Studies

The sensitivity of some polarization observables to contributions from resonances in the 1900 MeV/c$^2$ were studied. In particular, Fig. 8 shows model predictions for the double-polarization observable $\mathbf{P}_y^\odot$ and how it differs from the full solution (solid line) if for example the $S_{31}$ (1900) (dashed curves) or the $P_{31}$ (1910) (dot-dashed curves) are omitted from the calculation. The plot is largely independent of the photocouplings of the excited baryons, indicating the contributions in which the excited baryon couples to the proton is small. No baryons with spin greater than 3/2 have been included, but all resonances below 1.94 GeV/c$^2$ were considered.

Note that the observables are very sensitive to particular kinematic variables (like $\Phi$) (Fig. 9)and in some cases, exhibit large values. The conclusion from these investigations is that we should allow for an absolute error of 0.05 in order to study the 1900 MeV/c$^2$ mass region. In order to obtain this absolute error, four days of beam time were requested and granted.

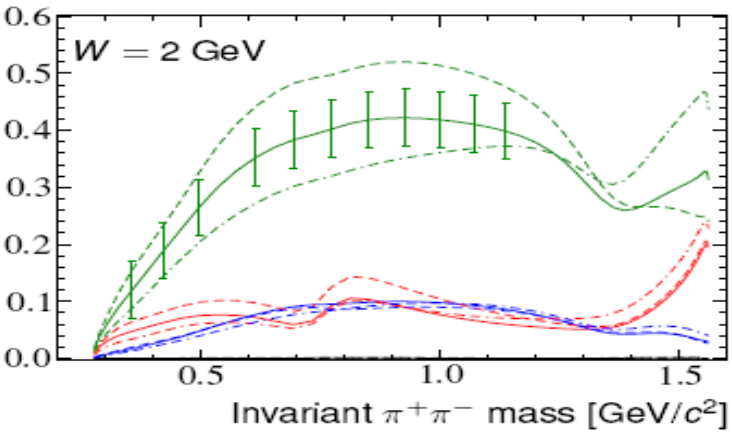


*Fig 8: Model calculations by W. Roberts for circularly-polarized beam and transverse target polarization [2]. The plot shows the predictions for the double-polarization observable $P_y^\odot$ versus the invariant mass of two of our final state particles, $\pi^+\pi^-$. The solid curves correspond to the full calculation, whereas the dashed curves arise when the $S_{31}(1900)$ is omitted from the calculations and the dot-dashed curves arise when the $P_{31}(1910)$ is omitted from the calculations. The black curves (which lie on the horizontal axis) are at $\Phi\approx 0$, the red curves are at $\Phi\approx 1/6\pi$, the green curves are at $\Phi\approx 2/3\pi$ and the blue curves are at $\Phi\approx\pi$.*

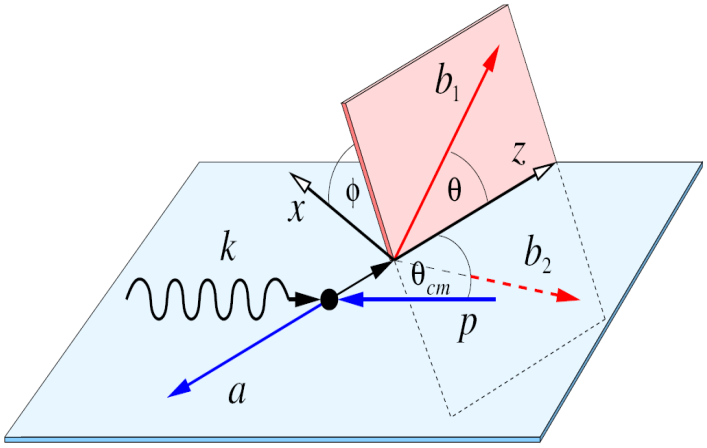


*Fig 9: Decay angles in a 3-particle final state in a center-of-mass frame. $\Phi$ is the angle between the production plane and the plane formed by two of the final state particles.*

## Summary

This experiment will serve to compliment the data taken by four other scheduled FROST experiments: E02-112, E03-105, E04-102, E05-012. This experiment will add four days of run time to the 84 days already awarded to FROST-related experiments in order to investigate photoproduced baryon resonances. The FSU Hadronic Spectroscopy Group will lead the analysis of the data from this double-pion photoproduction experiment. My thesis will involve the isolation and measurement of at least one polarization observable, depending on the run conditions. I will most likely be analyzing data from a circularly polarized photon beam incident on a longitudinally polarized target, depending on the quality of data. Construction of the FROST target will be complete November 2006 and tested in the target group workspace November/December 2006. I will be aiding in this testing which will involve leak-checking external of FROST in liquid nitrogen (77 K) and then the internal of FROST by pumping liquid $He_4$ at 1 K through it while the unit resides in a vacuum tube. It will then be disassembled, transported to Hall B, reassembled and then tested once more in the hall. This instillation in Hall B will occur in January 2007 with experimental runs beginning late February 2007.

## References


[1] U. Loring, K. Kretzschmar, B. Metsch, and H. Petry, "*Relativistic quark models of baryons with instantaneous forces*", Eur. Phys. J. A10, 309 (2001), hep-ph/0103287

[2] W. Roberts and A. Rakotovao, "*A model for two-pion photoproduction amplitudes*", (1997), hep-ph/9708236

[3] W. Roberts and T. Oed, *"Polarization Observables for Two-pion Production off the Nucleon"*, (2004), nucl-th/0410012

[4] H. Olsen and L. Maximon, Phys. Rev. **114**, 887 (1959)

[5] E02-112 : Search for Missing Nucleon Resonances in Hyperon Photoproduction http://www.jlab.org/exp_prog/CEBAF_EXP/E02112.html

[6] E03-105 : Pion Photoproduction from a Polarized Target http://www.jlab.org/exp_prog/CEBAF_EXP/E03105.html

[7] E04-102 : Helicity Structure of Pion Photoproduction http://www.jlab.org/exp_prog/CEBAF_EXP/E04102.html

[8] E05-012 : Measurement of polarization observables in $\eta$-photoproduction with CLAS http://www.jlab.org/exp_prog/CEBAF_EXP/E05012.html

[9] E06-013 : Measurement of $\pi^+\pi^-$ Photoproduction in Double-Polarization Experiments using CLAS http://www.jlab.org/exp_prog/CEBAF_EXP/E06013.html

[10] W. Meyer, Prepared for Symposium on the Gerasimov-Drell-Hearn Sum Rule and the Nucleon Spin Structure in the Resonance Region (GDH 2000), Mainz, Germany, 14-17 Jun 2000

[11] C. Bradtke *et al., "A new frozen-spin target for $4\pi$ particle detection"*, Nucl. Instrum. Meth. **A** 436, 430 (1999)

[12] S. Capstick and N. Isgur, *"Baryons in a Relativized Quark Model with Chromodynamics"*, Phys. Rev. **D34**, 2809 (1986)

[13] L. Glozman and D. Riska, *"The spectrum of the nucleons and the strange hyperons and chiral dynamics"*, Phys. Rept. **268**, 263 (1996), hep-ph/9505422